Supplementary Information

Structural Diversity of Supramolecular Networks Composed of 2,1,3-Chalcogenadiazole Silver(I) Complexes: The Role of Chalcogen Bonding in Molecular Self–Assembly

Jan Alfuth,[1] Jarosław Chojnacki,[2] Tadeusz Połoński,[1] Teresa Olszewska[1,*]

[1] Department of Organic Chemistry, Faculty of Chemistry, Gdańsk University of Technology, 80-233 Gdańsk, Poland.
[2] Department of Inorganic Chemistry, Faculty of Chemistry, Gdańsk University of Technology, 80-233 Gdańsk, Poland

** Corresponding author: phone: +48 58 347 14 25; e-mail: terolsze@pg.edu.pl*

Table of contents

Experimental procedures 3
IR spectra 5
X-Ray crystallography 9
References 21

Experimental procedures

The ligands **btd**, **bsd**, **4,5-dmbsd**, **5,6-dmbsd**, **ntd** and **nsd** were prepared following the literature procedures.[1–3]

4-methyl-2,1,3-benzoselenadiazole (**4-mbsd**)

In a round-bottom flask, 3-methylbenzene-1,2-diamine (611 mg, 5 mmol) was dissolved in 10 ml of anhydrous MeOH. The solution was heated to 40°C and then SeO_2 (1.11 g, 10 mmol, 2 eq) dissolved in 2 ml of anhydrous MeOH was added in one portion. The solvent was evaporated and the crude product was purified by column chromatography on silica gel using hexane/AcOEt (8:2) as eluent to give pure **4-mbsd** (771 mg, 3.91 mmol, 78%) as pale-yellow solid.
mp 108–111°C. ^{1}H NMR (500 MHz, $CDCl_3$): δ 7.67 (d, *J* = 9.1 Hz, 1H), 7.37 (dd, *J* = 9.0, 6.5 Hz, 1H), 7.20 (dd, *J* = 6.5, 1.1 Hz, 1H), 2.71 (s, 3H).

$[Ag_2$(**btd**)$(NO_3)_2]_n$ (**1a**)

In a round-bottom flask, **btd** (272 mg, 2 mmol) and $AgNO_3$ (170 mg, 1 mmol) were dissolved in a minimal amount of boiling acetonitrile. The solution was cooled to room temperature and then left to concentrate in the dark for several days to give colourless crystals.
mp 230–231°C (decomp.). Elem. Anal. Calcd for $C_6H_4Ag_2N_4O_6S$: C, 15.14; H, 0.85; N, 11.77; S, 6.74. Found: C, 15.28; H, 0.89; N, 11.85; S, 6.85.

$[Ag_2$(**bsd**)$(NO_3)_2]_n$ (**1b**)

In a round-bottom flask, **bsd** (549 mg, 3 mmol) and $AgNO_3$ (170 mg, 1 mmol) were dissolved in a minimal amount of boiling acetonitrile/water mixture. The solution was cooled to room temperature and then left to concentrate in the dark for several days to give colourless crystals.
mp 264–265°C (decomp.). Elem. Anal. Calcd for $C_6H_4Ag_2N_4O_6Se$: C, 13.78; H, 0.77; N, 10.72. Found: C, 13.90; H, 0.74; N, 10.56.

$[Ag($**4-mbsd**$)_2(NO_3)]$ (**2α** and **2β**)

To a solution of **4-mbsd** (394 mg, 2 mmol) in 7 ml of acetonitrile, a solution of $AgNO_3$ (170 mg, 1 mmol) in 7 ml was added after which small light-yellow needles of polymorph **2β** immediately appeared, which were collected and dried (mp 234–235°C).
When the crystals of **2β** were left in the mother liquor in the dark, they gradually changed their form into large colourless blocks of the second polymorph **2α** (mp 211–213°C).
Elem. Anal. Calcd for $C_{14}H_{12}AgN_5O_3Se_2$: C, 29.81; H, 2.14; N, 12.42. Found: C, 29.82; H, 2.16; N, 12.38.

$[Ag_2($**4,5-dmbsd**$)_4(\mu\text{-}NO_3)_2]$ (**3**)

In a round-bottom flask, **4,5-dmbsd** (211 mg, 1 mmol) and $AgNO_3$ (170 mg, 1 mmol) were dissolved in a minimal amount of boiling acetonitrile. The solution was cooled to room temperature and then left to concentrate in the dark for several days to give pale-yellow crystals.
mp 236–237°C. Elem. Anal. Calcd for $C_{16}H_{16}AgN_5O_3Se_2$: C, 32.45; H, 2.72; N, 11.83. Found: C, 32.42; H, 2.74; N, 11.79.

$[Ag(\mu$-**5,6-dmbsd**$)(H_2O)^+, NO_3^-]_n$ (**4**)

In a round-bottom flask, **4,5-dmbsd** (211 mg, 1 mmol) and $AgNO_3$ (170 mg, 1 mmol) were dissolved in a minimal amount of boiling acetonitrile. The solution was cooled to room temperature and then left to concentrate in the dark for several days to give light yellow crystals.
mp 214–215°C. Elem. Anal. Calcd for $C_8H_8AgN_3O_3Se{\cdot}H_2O$: C, 24.08; H, 2.53; N, 10.53. Found: C, 23.88; H, 2.49; N, 10.40.

$[Ag(\mu$-**ntd**$)(NO_3)]_n$ (**5a**)

In a round-bottom flask, **ntd** (186 mg, 1 mmol) and $AgNO_3$ (170 mg, 1 mmol) were dissolved in a minimal amount of boiling acetonitrile. The solution was cooled to room temperature and then left to concentrate in the dark for several days to give deep red crystals.
mp 174°C (decomp.). Elem. Anal. Calcd for $C_{10}H_6AgN_3O_3S$: C, 33.73; H, 1.70; N, 11.80; S, 9.00. Found: C, 33.62; H, 1.69; N, 11.78; S, 9.12.

[Ag(μ-**nsd**)(NO_3)]$_n$ (**5b**)

In a round-bottom flask, freshly prepared **ntd** (233 mg, 1 mmol) and $AgNO_3$ (170 mg, 1 mmol) were dissolved in a minimal amount of boiling acetonitrile. The solution was cooled to room temperature (and filtered if necessary) and then left to concentrate in the dark for several days to give dark burgundy crystals.
mp >320°C (decomp.). Elem. Anal. Calcd for $C_{10}H_6AgN_3O_3Se$: C, 29.80; H, 1.50; N, 10.43. Found: C, 30.17; H, 1.53; N, 10.38.

[Ag(**btd**)$_2$(H_2O)](BF_4) (**6a**)

In a round-bottom flask, **btd** (136 mg, 1 mmol) and $AgBF_4$ (195 mg, 1 mmol) were dissolved in a minimal amount of boiling acetonitrile. The solution was cooled to room temperature and then left to concentrate in the dark for several days to give colourless blocks.
mp 115–117°C. Elem. Anal. Calcd for $C_{12}H_8AgBF_4N_4S_2 \cdot H_2O$: C, 29.71; H, 2.08; N, 11.55. Found: C, 29.92; H, 2.15; N, 11.65.

[Ag(**bsd**)$_2$(MeCN)](BF_4) (**6b**)

In a round-bottom flask, **btd** (183 mg, 1 mmol) and $AgBF_4$ (195 mg, 1 mmol) were dissolved in a minimal amount of boiling acetonitrile. The solution was cooled to room temperature and then left to concentrate in the dark for several days to give yellow crystals.
mp 229°C (decomp.). Elem. Anal. Calcd for $C_{12}H_8AgBF_4N_4Se_2 \cdot CH_3CN$: C, 27.94; H, 1.84; N, 11.64. Found: C, 27.51; H, 1.81; N, 11.76.

[Ag(**bsd**)$_2$(MeCN)](SbF_6) (**7**)

In a round-bottom flask, **bsd** (183 mg, 1 mmol) and $AgSbF_6$ (344 mg, 1 mmol) were dissolved in a minimal amount of boiling acetonitrile. The solution was cooled to room temperature and then left to concentrate in the dark for several days to give light-yellow crystals.
mp 265°C (decomp.). Elem. Anal. Calcd for $(C_{12}H_8AgF_6N_4SbSe_2)_2 \cdot CH_3CN$: C, 21.38; H, 1.31; N, 8.63. Found: C, 21.35; H, 1.58; N, 8.78.

[Ag(**4,5-dmbsd**)$_2$](ClO_4)] (**8**)

In a round-bottom flask, **4,5-dmbsd** (211 mg, 1 mmol) and $AgClO_4$ (207 mg, 1 mmol) were dissolved in a minimal amount of boiling acetonitrile. The solution was cooled to room temperature and then left to concentrate in the dark for several days to give yellow small crystals.
mp 203°C (rapid decomp.). Elem. Anal. Calcd for $C_{16}H_{16}AgClN_4O_4Se_2$: C, 30.52; H, 2.56; N, 8.90. Found: C, 30.48; H, 2.54; N, 8.95.

[Ag(**ntd**)$_2$(MeCN)](ClO_4)] (**9a**)

In a round-bottom flask, **ntd** (186 mg, 1 mmol) and $AgClO_4$ (207 mg, 1 mmol) were dissolved in a minimal amount of boiling acetonitrile. The solution was cooled to room temperature and then left to concentrate in the dark for several days to give deep red crystals.
mp 241–244°C. Elem. Anal. Calcd for $(C_{20}H_{12}AgClN_4O_4S_2)_4 \cdot (CH_3CN)_3$: C, 42.20; H, 2.32; N, 10.77. Found: C, 41.48; H, 2.61; N, 10.82.

[Ag(**nsd**)$_2$(H_2O)$_2$](ClO_4) (**9b**)

In a round-bottom flask, freshly prepared **ntd** (233 mg, 1 mmol) and $AgClO_4$ (207 mg, 1 mmol) were dissolved in a minimal amount of boiling acetonitrile/water mixture. The solution was cooled to room temperature (and filtered if necessary) and then left to concentrate in the dark for several days to give dark burgundy crystals.
mp >320°C. Elem. Anal. Calcd for $(C_{20}H_{12}AgClN_4O_4Se_2)_3 \cdot (CH_3CN)_4$: C, 37.38; H, 2.21; N, 10.26. Found: C, 37.71; H, 2.23; N, 10.12.

IR spectra

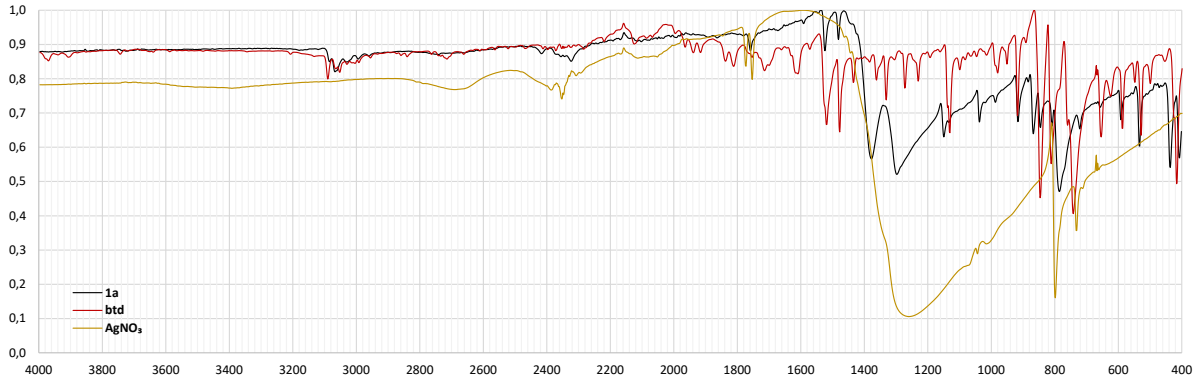

Figure S1. Solid-state IR spectra of **1a**, **btd** and $AgNO_3$.

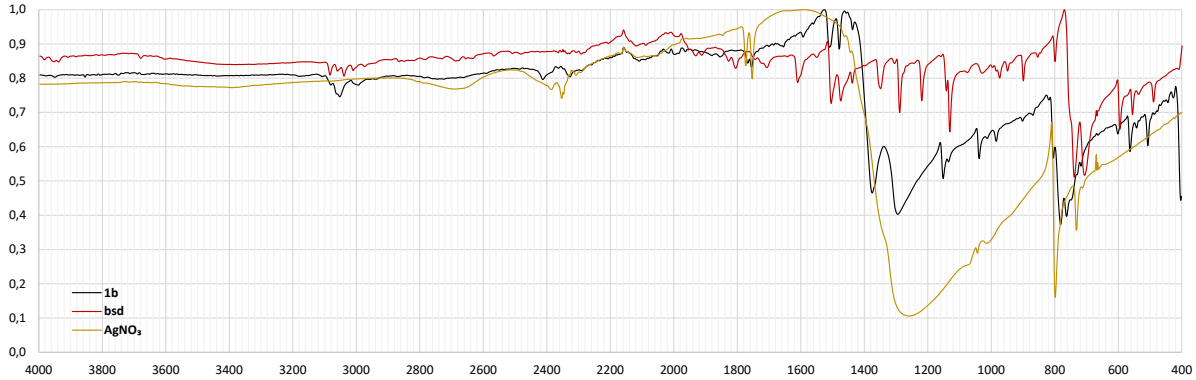

Figure S2. Solid-state IR spectra of **1b**, **bsd** and $AgNO_3$.

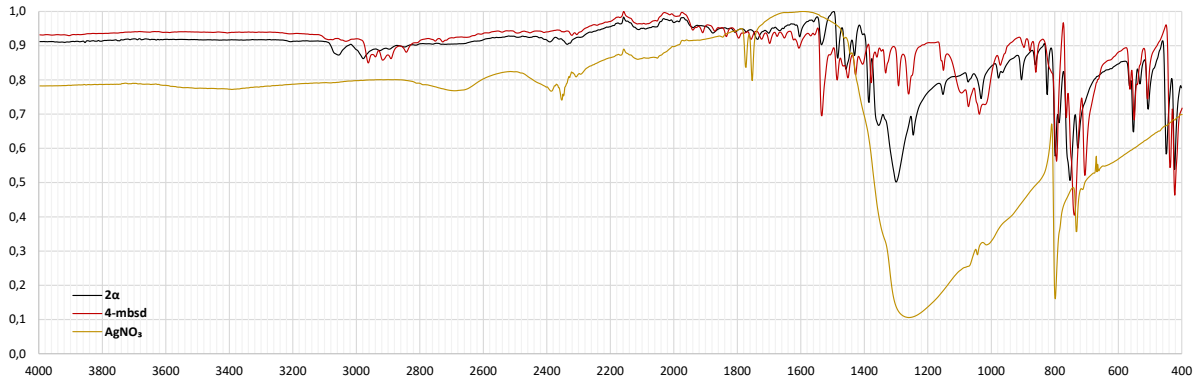

Figure S3. Solid-state IR spectra of **2α**, **4-mbsd** and $AgNO_3$.

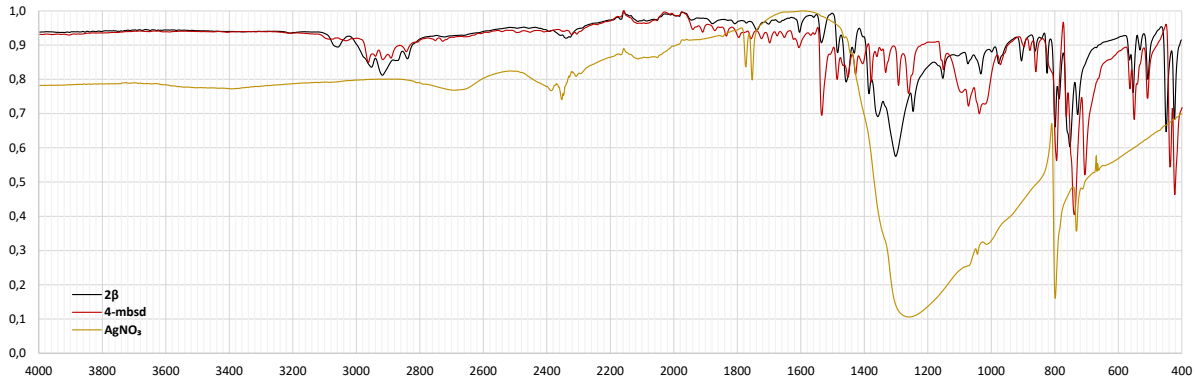

Figure S4. Solid-state IR spectra of **2β**, **4-mbsd** and $AgNO_3$.

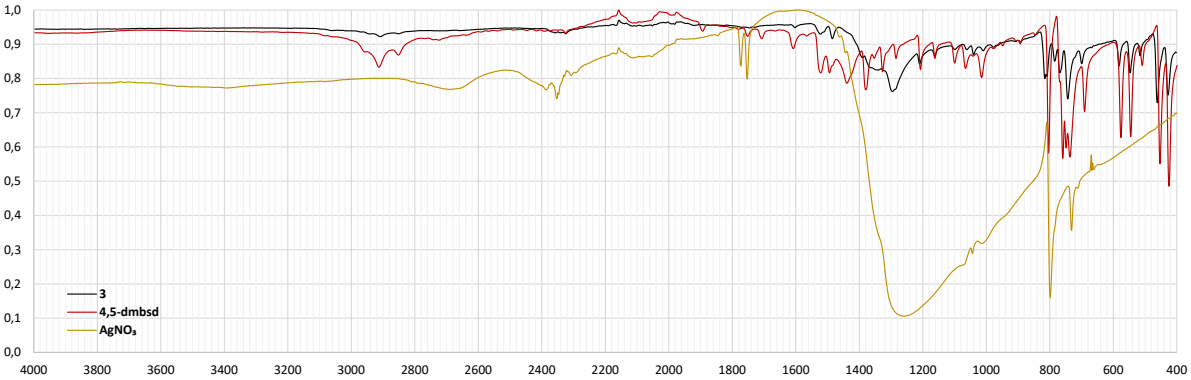

Figure S5. Solid-state IR spectra of **3** and **4,5-dmbsd** and $AgNO_3$.

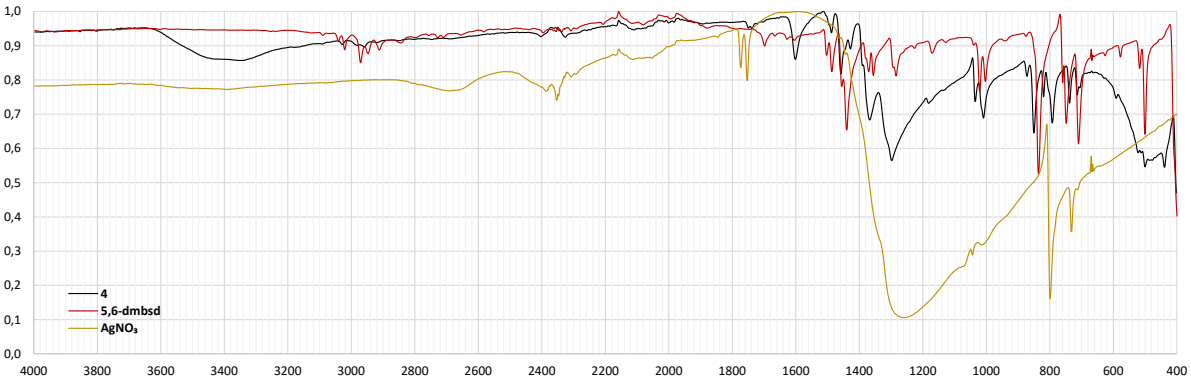

Figure S6. Solid-state IR spectra of **4** and **5,6-dmbsd** and $AgNO_3$.

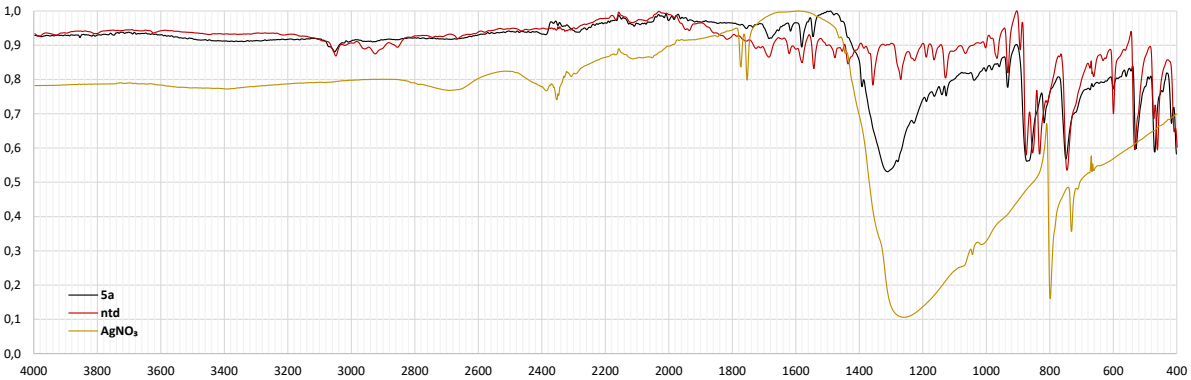

Figure S7. Solid-state IR spectra of **5a** and **ntd** and $AgNO_3$.

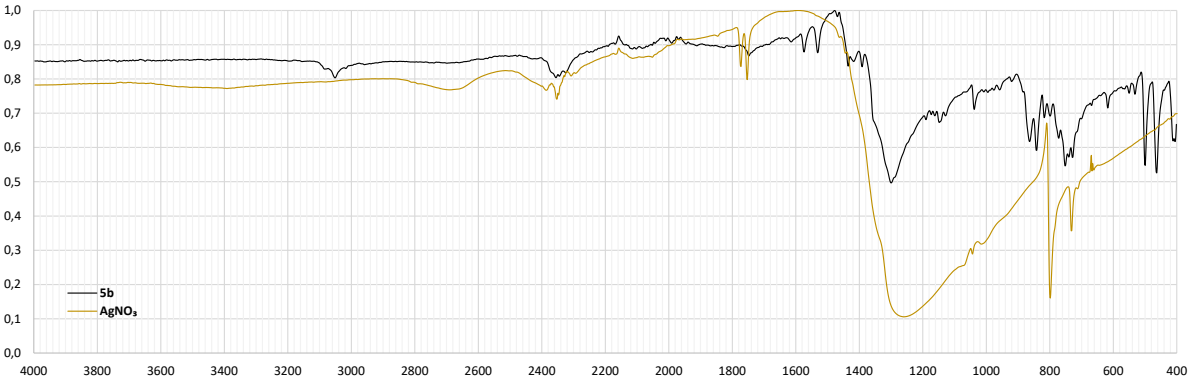

Figure S8. Solid-state IR spectrum of **5b** and $AgNO_3$.

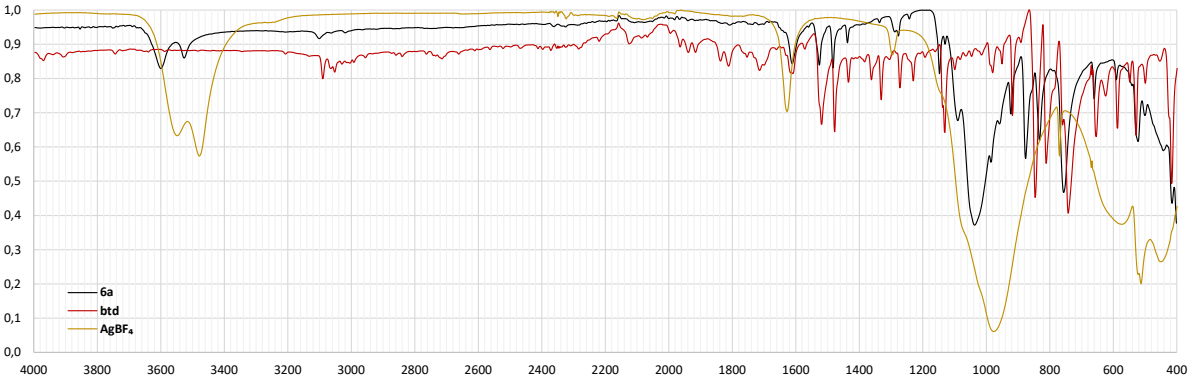

Figure S9. Solid-state IR spectra of **6a** and **btd** and $AgBF_4$.

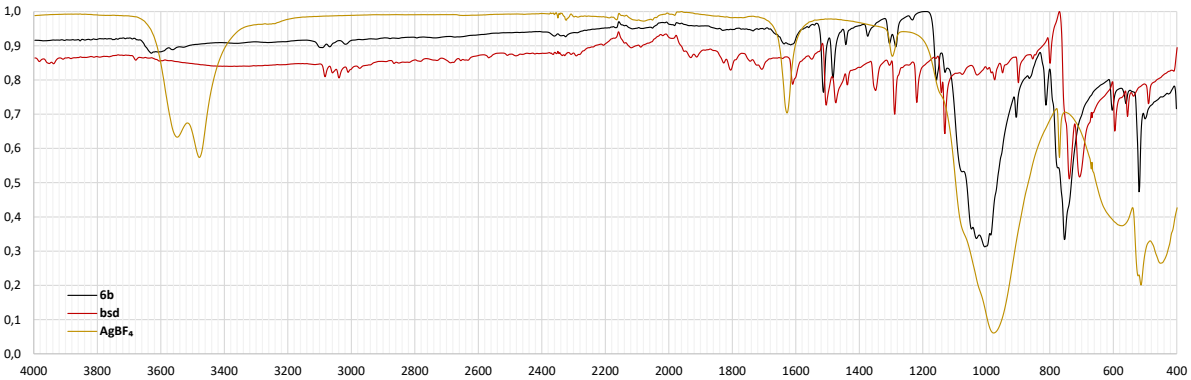

Figure S10. Solid-state IR spectra of **6b** and **bsd** and $AgBF_4$.

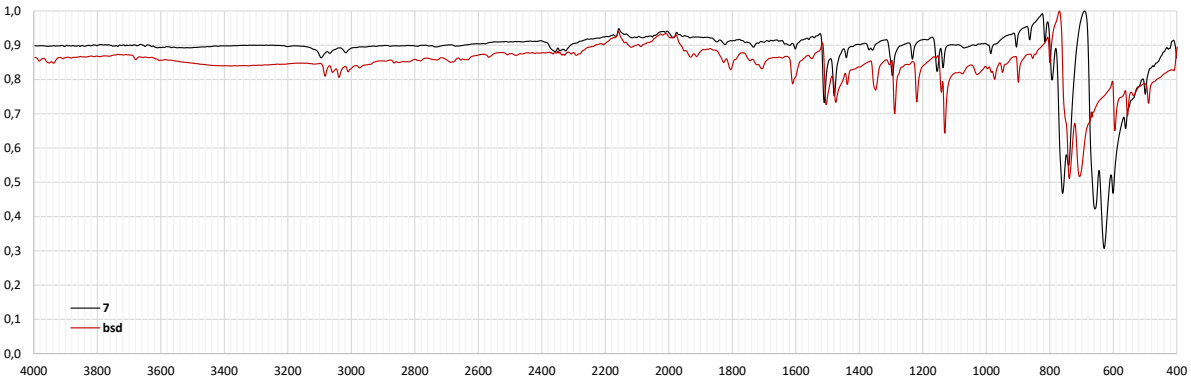

Figure S11. Solid-state IR spectra of **7** and **bsd** and $AgSbF_6$.

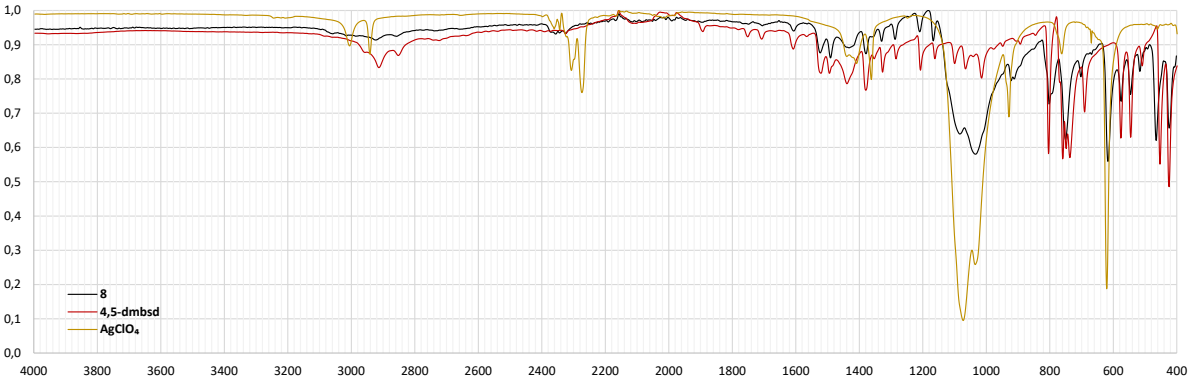

Figure S12. Solid-state IR spectra of **8** and **4,5-dmbsd** and $AgClO_4$.

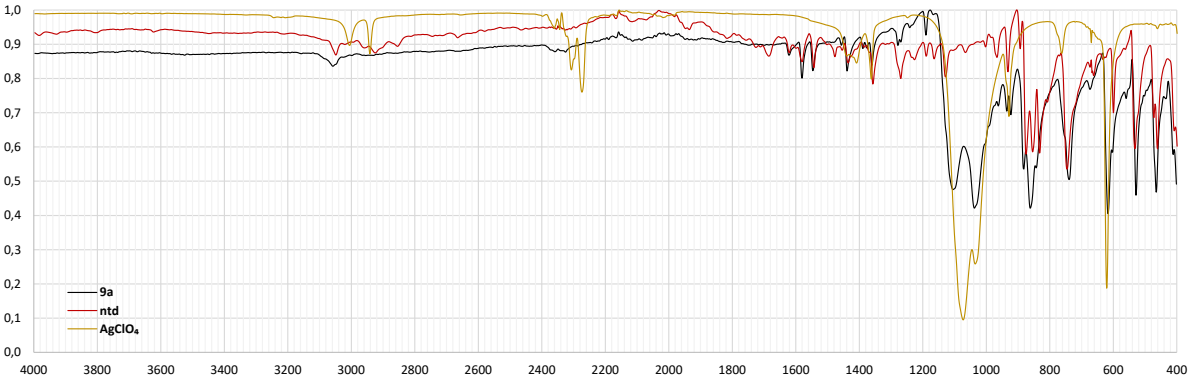

Figure S13. Solid-state IR spectra of **9a** and **ntd** and $AgClO_4$.

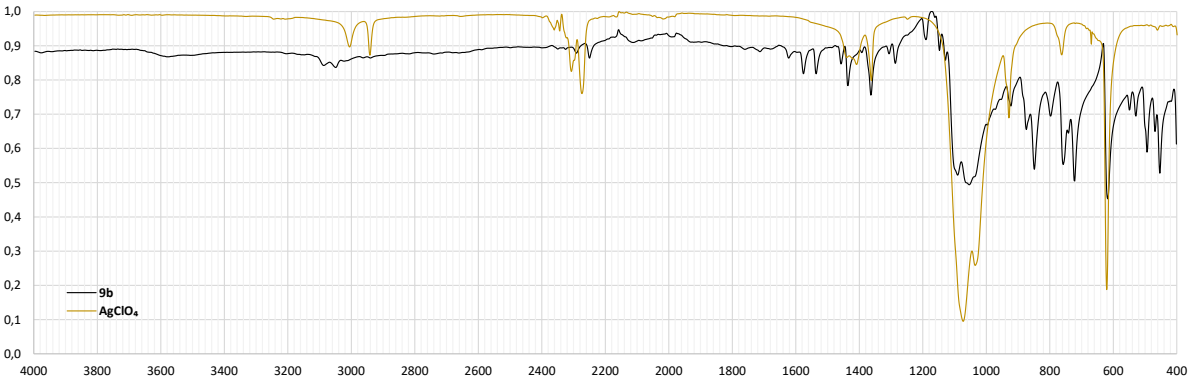

Figure S14. Solid-state IR spectrum of **9b** and $AgClO_4$.

X-Ray crystallography

Table S1. Crystal data, data collection and structure refinement details for all complexes.

	1a	**1b**	**2α**	**2β**
CCDC deposition number	2485236	2485237	2485238	2485239
Crystal data				
Chemical formula	$C_6H_4Ag_2N_4O_6S$	$C_6H_4Ag_2N_4O_6Se$	$C_{14}H_{12}AgN_5O_3Se_2$	$C_{28}H_{24}Ag_2N_{10}O_6Se_4$
Formula weight (g mol^{-1})	475.93	522.83	564.08	1128.15
Crystal system	Monoclinic	Monoclinic	Triclinic	Monoclinic
Space group	*I*2/*a*	*I*2/*a*	$P\bar{1}$	$P2_1/c$
Temperature (K)	120	120	120	120
a (Å)	7.201(3)	7.1843(5)	7.3648(8)	7.456(4)
b (Å)	9.608(4)	9.6347(4)	9.9357(11)	21.169(11)
c (Å)	15.507(8)	15.7023(11)	11.3068(14)	11.074(5)
α (°)	90	90	96.414(9)	90
β (°)	103.18(4)	102.367(6)	91.408(9)	109.36(3)
γ (°)	90	90	104.754(9)	90
Volume (Å^3)	1044.6(9)	1061.67(12)	793.87(16)	1648.9(14)
Z	4	4	2	2
Radiation type	Mo K*α*	Mo K*α*	Mo K*α*	Mo K*α*
μ (mm^{-1})	3.98	7.15	5.88	5.66
Crystal size (mm)	0.34 × 0.12 × 0.06	0.11 × 0.07 × 0.03	0.53 × 0.22 × 0.17	0.26 × 0.02 × 0.02
Data collection				
Diffractometer	STOE IPDS 2T	STOE IPDS 2T	STOE IPDS 2T	STOE IPDS 2T
Absorption correction	*A (see below)*	*A (see below)*	*A (see below)*	*A (see below)*
T_{min}, T_{max}	0.470, 0.792	0.468, 0.866	0.087, 0.367	0.463, 0.923
No. of measured, independent and observed [$I>2\sigma(I)$] reflections	3411, 1411, 1315	6536, 1436, 1352	10944, 4273, 3881	6707, 2925, 1746
R_{int}	0.023	0.026	0.027	0.109
$(\sin\theta/\lambda)_{max}$ (Å^{-1})	0.685	0.686	0.686	0.597
Refinement				
$R[F^2 > 2\sigma(F^2)]$, $wR(F^2)$, S	0.024, 0.065, 1.04	0.025, 0.069, 1.08	0.032, 0.087, 1.05	0.089, 0.252, 1.02
No. of reflections	1411	1436	4273	2925
No. of parameters	88	87	228	228
No. of restraints	0	0	0	0
H-atom treatment	H-atom parameters constrained $w = 1/[\sigma^2(F_o^2) + (0.0495P)^2 + 0.4077P]$ where $P = (F_o^2 + 2F_c^2)/3$	H-atom parameters constrained $w = 1/[\sigma^2(F_o^2) + (0.0425P)^2 + 3.3774P]$ where $P = (F_o^2 + 2F_c^2)/3$	H-atom parameters constrained $w = 1/[\sigma^2(F_o^2) + (0.0563P)^2 + 0.7653P]$ where $P = (F_o^2 + 2F_c^2)/3$	H-atom parameters constrained $w = 1/[\sigma^2(F_o^2) + (0.1029P)^2 + 39.8179P]$ where $P = (F_o^2 + 2F_c^2)/3$
$\Delta\rangle_{max}$, $\Delta\rangle_{min}$ (e Å^{-3})	0.79, –0.99	0.80, –0.66	0.84, –1.36	1.35, –1.05

Absorption correction A: Integration
STOE X-RED32, absorption correction by Gaussian integration, analogous to P. Coppens, "*The Evaluation of Absorption and Extinction in Single-Crystal Structure Analysis*", published in F. R. Ahmed (Editor), "*Crystallographic Computing*", Munksgaard, Copenhagen (**1970**), 255–270.

Table S1. *(continued)* Crystal data, data collection and structure refinement details for all structures.

	3	**4**	**5a**	**5b**
CCDC deposition number	2485240	2485241	2485242	2485243
Crystal data				
Chemical formula	$C_{16}H_{16}AgN_5O_3Se_2$	$C_8H_8AgN_2Se{\cdot}NO_3{\cdot}H_2O$	$C_{30}H_{18}Ag_3N_9O_9S_3$	$C_{10}H_6AgN_3O_3Se$
Formula weight (g mol^{-1})	592.13	399.02	1068.32	403.01
Crystal system	Monoclinic	Orthorhombic	Monoclinic	Monoclinic
Space group	$P2_1/n$	$Pbca$	$P2_1/c$	$P2/n$
Temperature (K)	120	120	120	120
a (Å)	7.0765(18)	13.3558(5)	6.7953(4)	6.880(2)
b (Å)	14.922(3)	7.1039(3)	35.947(2)	12.017(5)
c (Å)	17.437(3)	23.5974(14)	13.5656(8)	6.9630(19)
α (°)	90	90	90	90
β (°)	98.577(18)	90	101.474(5)	117.27(2)
γ (°)	90	90	90	90
Volume (Å^3)	1820.7 (7)	2238.88 (18)	3247.5 (3)	511.7 (3)
Z	4	8	4	2
Radiation type	Mo Kα	Mo Kα	Mo Kα	Mo Kα
μ (mm^{-1})	5.13	5.06	2.06	5.53
Crystal size (mm)	0.29 × 0.03 × 0.02	0.54 × 0.12 × 0.04	0.02 (radius)	0.12 × 0.06 × 0.02
Data collection				
Diffractometer	STOE IPDS 2T	STOE IPDS 2T	STOE IPDS 2T	STOE IPDS 2T
Absorption correction	*A (see below)*	*A (see below)*	*B (see below)*	*A (see below)*
T_{min}, T_{max}	0.323, 0.896	0.461, 0.913	0.388, 0.698	0.464, 0.839
No. of measured, independent and observed [$I>2\sigma(I)$] reflections	3567, 3567, 3071	10544, 2199, 1862	52427, 8793, 7720	5046, 1016, 872
R_{int}	*merged*	0.059	0.026	0.089
(sin $\theta/\lambda)_{max}$ (Å^{-1})	0.618	0.617	0.687	0.616
Refinement				
$R[F^2 > 2\sigma(F^2)]$, $wR(F^2)$, S	0.125, 0.352, 1.26	0.076, 0.201, 1.11	0.037, 0.100, 1.09	0.076, 0.202, 1.06
No. of reflections	3567	2199	8793	1016
No. of parameters	239	163	487	84
No. of restraints	0	2	0	0
H-atom treatment	H-atom parameters constrained	H atoms treated by a mixture of independent and constrained refinement	H-atom parameters constrained	H-atom parameters constrained
	$w = 1/[\sigma^2(F_o^2) + 211.6686P]$ where $P = (F_o^2 + 2F_c^2)/3$	$w = 1/[\sigma^2(F_o^2) + (0.135P)^2 + 14.3992P]$ where $P = (F_o^2 + 2F_c^2)/3$	$w = 1/[\sigma^2(F_o^2) + (0.0436P)^2 + 9.8578P]$ where $P = (F_o^2 + 2F_c^2)/3$	$w = 1/[\sigma^2(F_o^2) + (0.1614P)^2 + 0.254P]$ where $P = (F_o^2 + 2F_c^2)/3$
$\Delta\rangle_{max}$, $\Delta\rangle_{min}$ (e Å^{-3})	2.73, –3.28	3.39, –3.73	0.65, –1.36	2.83, –1.60

Absorption correction A: Integration
STOE X-RED32, absorption correction by Gaussian integration, analogous to P. Coppens, "*The Evaluation of Absorption and Extinction in Single-Crystal Structure Analysis*", published in F. R. Ahmed (Editor), "*Crystallographic Computing*", Munksgaard, Copenhagen (**1970**), 255–270.

Absorption correction B: Multi-scan
STOE X-RED32, absorption correction by Gaussian integration, analogous to P. Coppens in: F. R. Ahmed (Editor), "*Crystallographic Computing*", Munksgaard, Copenhagen (**1970**), 255–270. Afterwards scaling of reflection intensities was performed within STOE LANA. J. Koziskova, F. Hahn, J. Richter, J. Kozisek, *Acta Chimica Slovaca*, Vol. 9, No. 2, **2016**, pp. 136–140. Finally a spherical absorption correction was done within STOE LANA.

Table S1. *(continued)* Crystal data, data collection and structure refinement details for all structures.

	6a	**6b**	**7**	**8**
CCDC deposition number	2485244	2485245	2485246	2485247
Crystal data				
Chemical formula	$C_{12}H_{10}AgN_4OS_2^+ \cdot BF_4^-$	$C_{12}H_8AgN_4Se_2^+ \cdot BF_4^- \cdot C_2H_3N$	$C_{12}H_8AgN_4Se_2^+ \cdot SbF_6^- \cdot C_2H_3N$	$C_{16}H_{16}AgN_4Se_2^+ \cdot ClO_4^-$
Formula weight (g mol^{-1})	485.04	601.88	750.82	629.57
Crystal system	Monoclinic	Triclinic	Monoclinic	Triclinic
Space group	$P2_1$	$P\bar{1}$	$P2_1/c$	$P\bar{1}$
Temperature (K)	120	120	120	120
a (Å)	6.9919(4)	7.8775(5)	12.2862(4)	7.4239(19)
b (Å)	11.3238(6)	10.6277(6)	10.8853(3)	13.407(4)
c (Å)	10.4854(5)	12.0636(7)	15.1578(5)	20.291(5)
α (°)	90	68.860(4)	90	107.42(2)
β (°)	106.456(4)	88.968(5)	100.846(3)	98.47(2)
γ (°)	90	69.456(5)	90	93.08(2)
Volume (Å^3)	796.17(7)	875.25(10)	1990.98(11)	1895.6(9)
Z	2	2	4	4
Radiation type	Mo Kα	Mo Kα	Mo Kα	Mo Kα
μ (mm^{-1})	1.58	5.36	6.06	5.08
Crystal size (mm)	0.24 × 0.12 × 0.09	0.14 × 0.09 × 0.04	0.14 × 0.07 × 0.05	0.21 × 0.15 × 0.03
Data collection				
Diffractometer	STOE IPDS 2T	STOE IPDS 2T	STOE IPDS 2T	STOE IPDS 2T
Absorption correction	*C (see below)*	*A (see below)*	*A (see below)*	*A (see below)*
T_{min}, T_{max}	0.335, 0.938	0.451, 0.851	0.416, 0.793	0.405, 0.885
No. of measured, independent and observed [$I>2\sigma(I)$] reflections	11080, 4042, 3965	12180, 4706, 3925	26301, 5368, 4840	16208, 6804, 5567
R_{int}	0.029	0.023	0.020	0.057
$(\sin\theta/\lambda)_{max}$ (Å^{-1})	0.688	0.688	0.694	0.599
Refinement				
$R[F^2 > 2\sigma(F^2)]$, $wR(F^2)$, S	0.021, 0.055, 1.03	0.038, 0.096, 1.15	0.024, 0.057, 1.06	0.101, 0.234, 1.18
No. of reflections	4042	4706	5368	6804
No. of parameters	227	245	263	513
No. of restraints	1	0	0	0
H-atom treatment	H-atom parameters constrained $w = 1/[\sigma^2(F_o^2) + (0.0336P)^2 + 0.441P]$ where $P = (F_o^2 + 2F_c^2)/3$	H-atom parameters constrained $w = 1/[\sigma^2(F_o^2) + (0.0206P)^2 + 6.1345P]$ where $P = (F_o^2 + 2F_c^2)/3$	H-atom parameters constrained $w = 1/[\sigma^2(F_o^2) + (0.0231P)^2 + 5.8385P]$ where $P = (F_o^2 + 2F_c^2)/3$	H-atom parameters constrained $w = 1/[\sigma^2(F_o^2) + (0.0001P)^2 + 112.0823P]$ where $P = (F_o^2 + 2F_c^2)/3$
$\Delta\rangle_{max}$, $\Delta\rangle_{min}$ (e Å^{-3})	0.73, –0.38	0.69, –0.97	0.58, –0.85	2.06, –1.31
Absolute structure	Flack x determined using 1708 quotients [(I+)-(I-)]/[(I+)+(I-)][S4]	–	–	–
Absolute structure parameter	0.206 (15)	–	–	–

Absorption correction A: Integration
STOE X-RED32, absorption correction by Gaussian integration, analogous to P. Coppens, "*The Evaluation of Absorption and Extinction in Single-Crystal Structure Analysis*", published in F. R. Ahmed (Editor), "*Crystallographic Computing*", Munksgaard, Copenhagen (**1970**), 255–270.

Absorption correction C: Multi-scan
STOE LANA, absorption correction by scaling of reflection intensities. J. Koziskova, F. Hahn, J. Richter, J. Kozisek, "*Comparison of different absorption corrections on the model structure of tetrakis(μ_2-acetato)-diaqua-di-copper(II)*", *Acta Chimica Slovaca*, Vol. 9, No. 2, **2016**, pp. 136-140. Afterwards a spherical absorption correction was performed within STOE LANA.

Table S1. *(continued)* Crystal data, data collection and structure refinement details for all structures.

	9a	**9b**
CCDC deposition number	2485248	2485249
Crystal data		
Chemical formula	$C_{22}H_{15}AgN_5S_2^+ \cdot ClO_4^-$	$C_{20}H_{14}AgN_4OSe_2^+ \cdot ClO_4^-$
Formula weight (g mol^{-1})	620.83	691.59
Crystal system	Triclinic	Triclinic
Space group	$P\bar{1}$	$P\bar{1}$
Temperature (K)	120	120
a (Å)	7.4983(10)	3.8140(4)
b (Å)	9.4191(12)	10.3541(10)
c (Å)	16.203(2)	14.2499(14)
α (°)	91.584(10)	92.620(8)
β (°)	90.423(10)	95.335(8)
γ (°)	104.261(10)	94.139(8)
Volume (Å^3)	1108.6(3)	558.06(10)
Z	2	1
Radiation type	Mo K*α*	Mo K*α*
μ (mm^{-1})	1.26	4.33
Crystal size (mm)	0.28 × 0.19 × 0.11	0.14 × 0.08 × 0.02
Data collection		
Diffractometer	STOE IPDS 2T	STOE IPDS 2T
Absorption correction	*B (see below)*	*A (see below)*
T_{min}, T_{max}	0.588, 0.817	0.586, 0.921
No. of measured, independent and observed [$I>2\sigma(I)$] reflections	21861, 5978, 5563	7736, 3004, 2110
R_{int}	0.021	0.041
$(\sin\theta/\lambda)_{max}$ (Å^{-1})	0.689	0.688
Refinement		
$R[F^2 > 2\sigma(F^2)]$, $wR(F^2)$, S	0.034, 0.092, 1.06	0.059, 0.157, 1.06
No. of reflections	5978	3004
No. of parameters	317	172
No. of restraints	0	2
H-atom treatment	H-atom parameters constrained $w = 1/[\sigma^2(F_o^2) + (0.0466P)^2 + 2.1149P]$ where $P = (F_o^2 + 2F_c^2)/3$	H-atom parameters constrained $w = 1/[\sigma^2(F_o^2) + (0.0638P)^2 + 3.7442P]$ where $P = (F_o^2 + 2F_c^2)/3$
$\Delta\rangle_{max}$, $\Delta\rangle_{min}$ (e Å^{-3})	1.17, –1.01	1.11, –1.06

Absorption correction A: Integration
STOE X-RED32, absorption correction by Gaussian integration, analogous to P. Coppens, "*The Evaluation of Absorption and Extinction in Single-Crystal Structure Analysis*", published in F. R. Ahmed (Editor), "*Crystallographic Computing*", Munksgaard, Copenhagen (**1970**), 255–270.

Absorption correction B: Multi-scan
STOE X-RED32, absorption correction by Gaussian integration, analogous to P. Coppens in: F. R. Ahmed (Editor), "*Crystallographic Computing*", Munksgaard, Copenhagen (**1970**), 255–270. Afterwards scaling of reflection intensities was performed within STOE LANA. J. Koziskova, F. Hahn, J. Richter, J. Kozisek, *Acta Chimica Slovaca*, Vol. 9, No. 2, **2016**, pp. 136–140. Finally a spherical absorption correction was done within STOE LANA.

Table S2. A summary of geometrical parameters of Ag–N and Ag–O bonds.

Complex	Ag–Y	$d_{Ag–Y}$ (Å)	symmetry codes i
1a	Ag1–N1	2.231(2)	
	Ag1–O1	2.281(2)	
	Ag1–O2^{i}	2.462(2)	1 – *x*, –0.5 + *y*, 0.5 – *z*
1b	Ag1–N1	2.200(3)	
	Ag1–O1	2.272(2)	
	Ag1–O2^{i}	2.460(2)	1 – *x*, –0.5 + *y*, 0.5 – *z*
2α	Ag1–N1	2.176(2)	
	Ag1–N2	2.169(2)	
	Ag1–O1	2.703(2)	
	Ag1–O3^{i}	2.869(2)	1 + *x*, *y*, *z*
2β	Ag1–N1	2.17(2)	
	Ag1–N3	2.17(1)	
	Ag1–O1	2.64(1)	
	Ag1–O3	2.67(1)	
	Ag1–O3^{i}	2.85(2)	1 – *x*, –*y*, 1 – *z*
3	Ag1–N1	2.24(2)	
	Ag1–N4	2.21(2)	
	Ag1–O1	2.65(2)	
	Ag1–O3^{i}	2.53(3)	1 – *x*, 1 – *y*, 1 – *z*
4	Ag1–N1	2.154(7)	
	Ag1–N2^{i}	2.197(7)	–0.5 + *x*, *y*, 1.5 – *z*
	Ag1–O4	2.618(7)	
	Ag1–O1	2.731(6)	
	Ag1–O1^{i}	2.938(7)	1 – *x*, –0.5 + *y*, 1.5 – *z*
5a	Ag1–N1	2.257(3)	
	Ag1–N2^{i}	2.279(3)	*x*, 0.5 – *y*, 0.5 + *z*
	Ag2–N3	2.263(3)	
	Ag3–N4	2.211(3)	
	Ag3–N5	2.193(3)	
	Ag2–N6^{i}	2.340(3)	*x*, *y*, –1 + *z*
	Ag1–O1	2.588(3)	
	Ag1–O4	2.626(3)	
	Ag2–O6	2.494(3)	
	Ag2–O7	2.470(3)	
	Ag3–O3^{i}	2.695(3)	*x*, 0.5 – *y*, 0.5 + *z*
	Ag3–O9^{i}	2.608(3)	1 – *x*, 1 – *y*, 1 – *z*
5b	Ag1–N1	2.261(6)	
	Ag1–O1	2.548(7)	
6a	Ag1–N1	2.159(3)	
	Ag1–N3	2.169(3)	
	Ag1–O1	2.586(3)	
6b	Ag1–N1	2.151(4)	
	Ag1–N3	2.142(4)	
	Ag1–N5	2.691(5)	
7	Ag1–N1	2.170(2)	
	Ag1–N3	2.183(2)	
	Ag1–N5	2.713(3)	
8	Ag1–N1	2.16(1)	
	Ag1–N3	2.18(1)	
	Ag1–N5	2.16(1)	
	Ag1–N7	2.18(1)	
9a	Ag1–N1	2.279(2)	
	Ag1–N3	2.289(2)	
	Ag1–N5	2.331(2)	
9b	Ag1–N1	2.162(5)	
	Ag1–O1W	2.636(16)	
	Ag1–O1	3.206(13)	

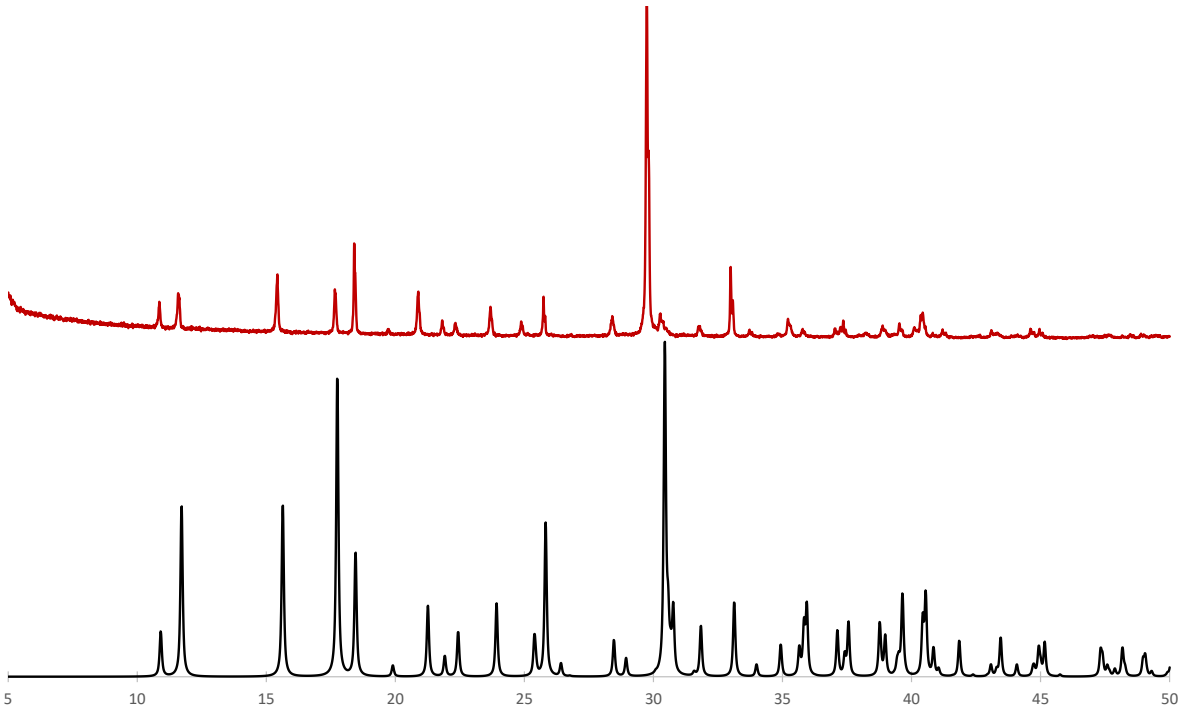

Figure S15. Experimental (red) and simulated (black) PXRD patterns of **1a**.

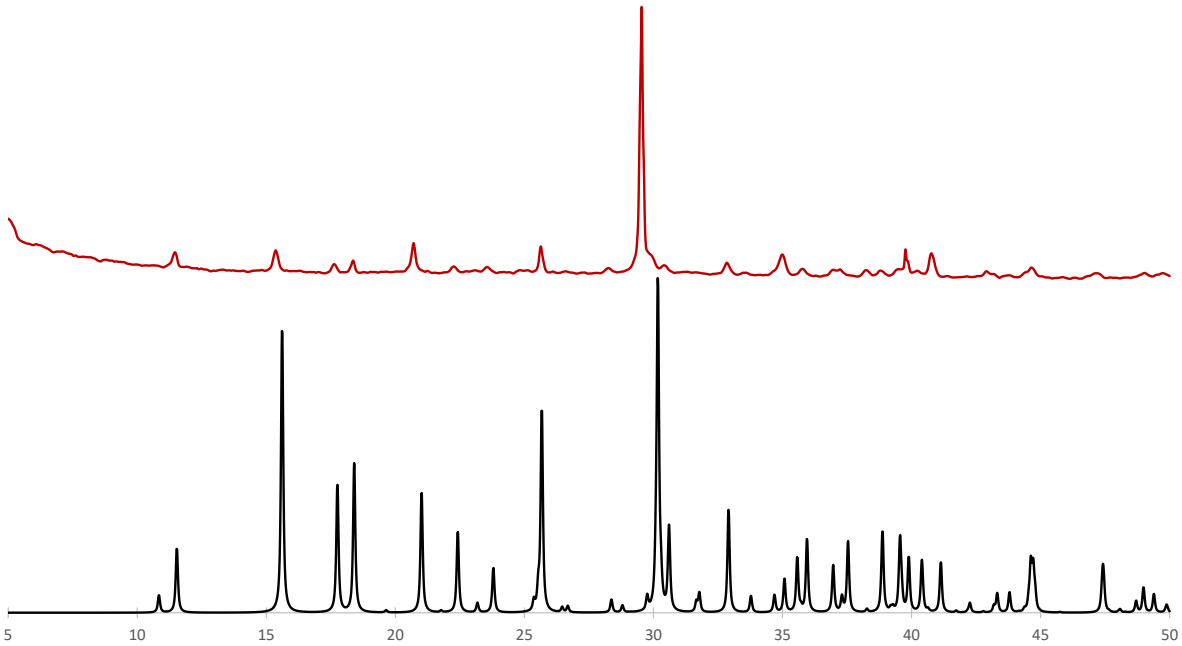

Figure S16. Experimental (red) and simulated (black) PXRD patterns of **1b**.

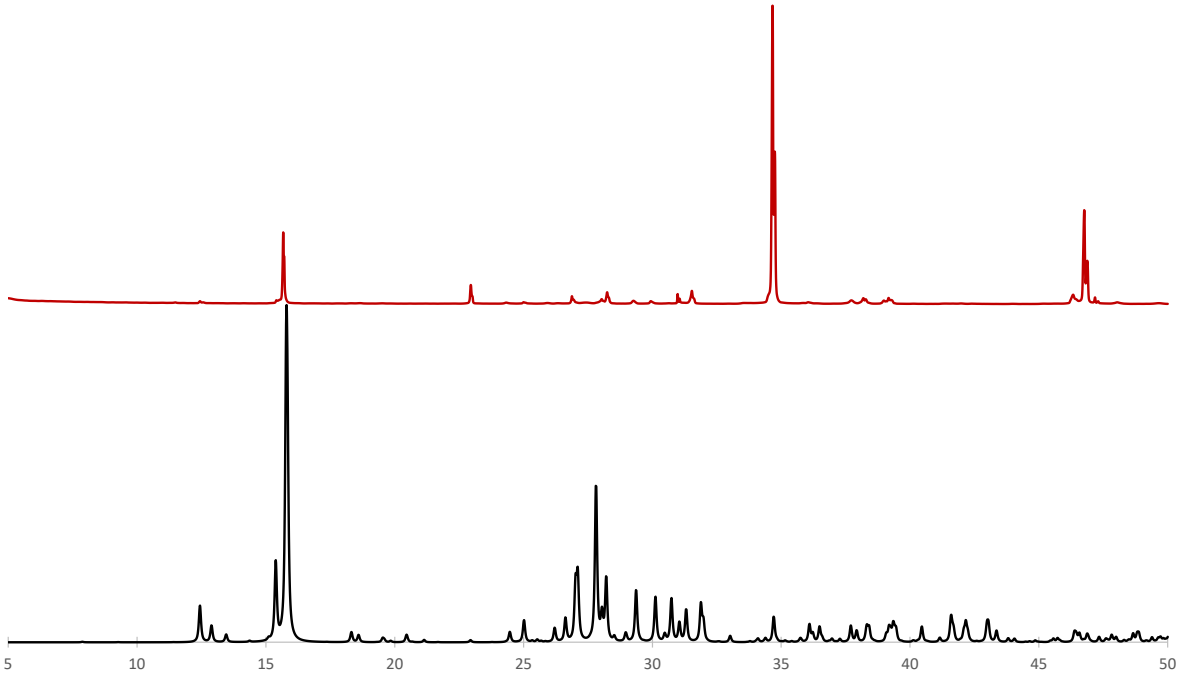

Figure S17. Experimental (red) and simulated (black) PXRD patterns of **2α**.

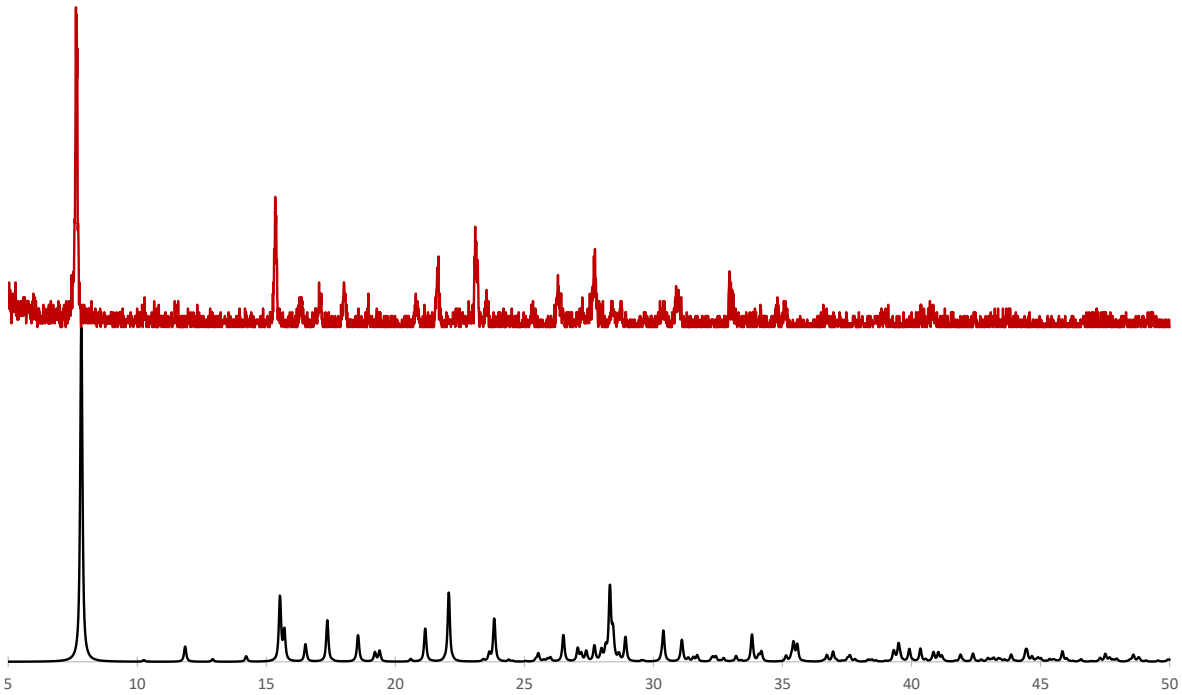

Figure S18. Experimental (red) and simulated (black) PXRD patterns of **3**.

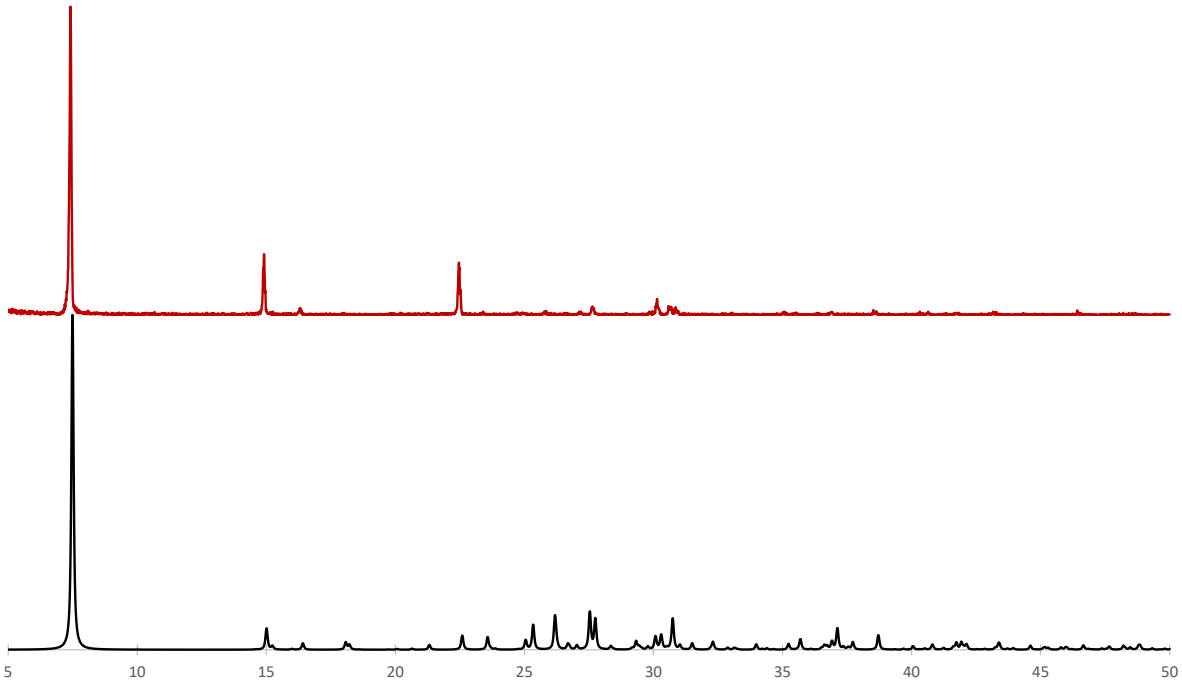

Figure S19. Experimental (red) and simulated (black) PXRD patterns of **4**.

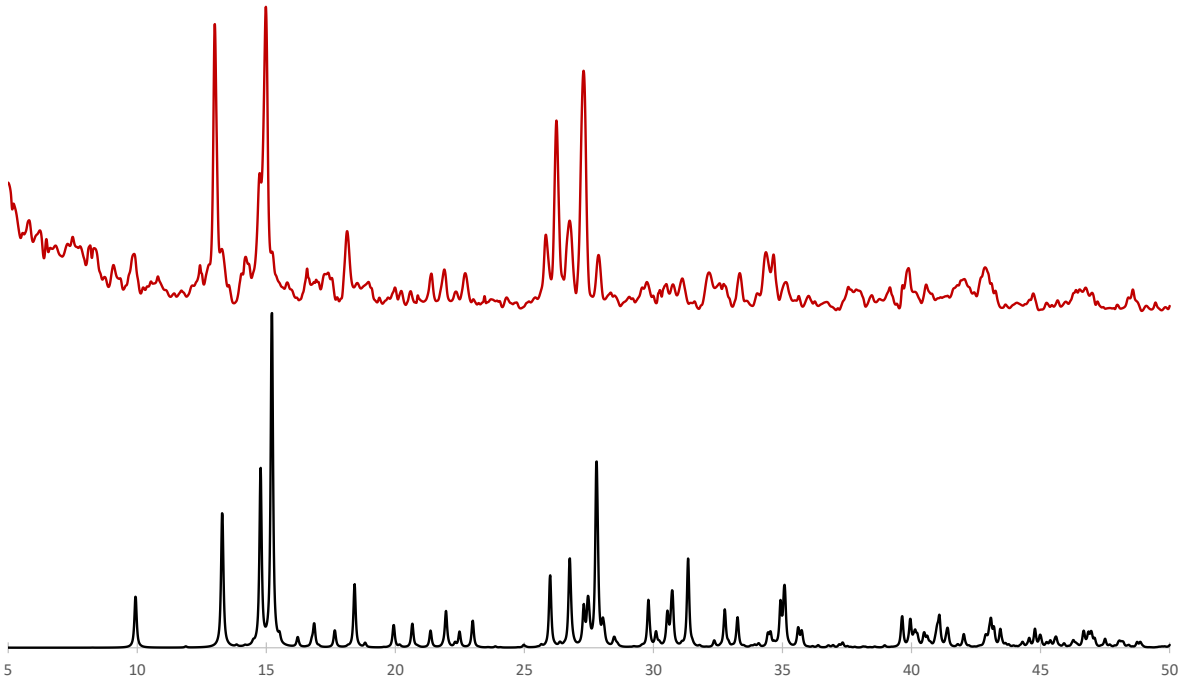

Figure S20. Experimental (red) and simulated (black) PXRD patterns of **5a**.

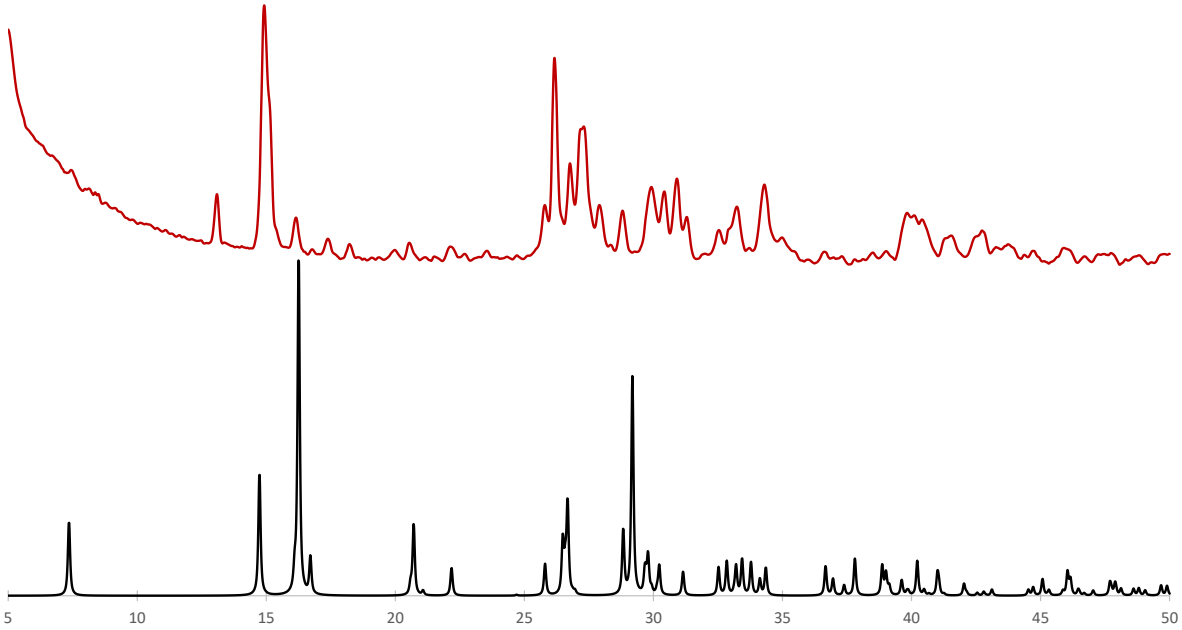

Figure S21. Experimental (red) and simulated (black) PXRD patterns of **5b**.

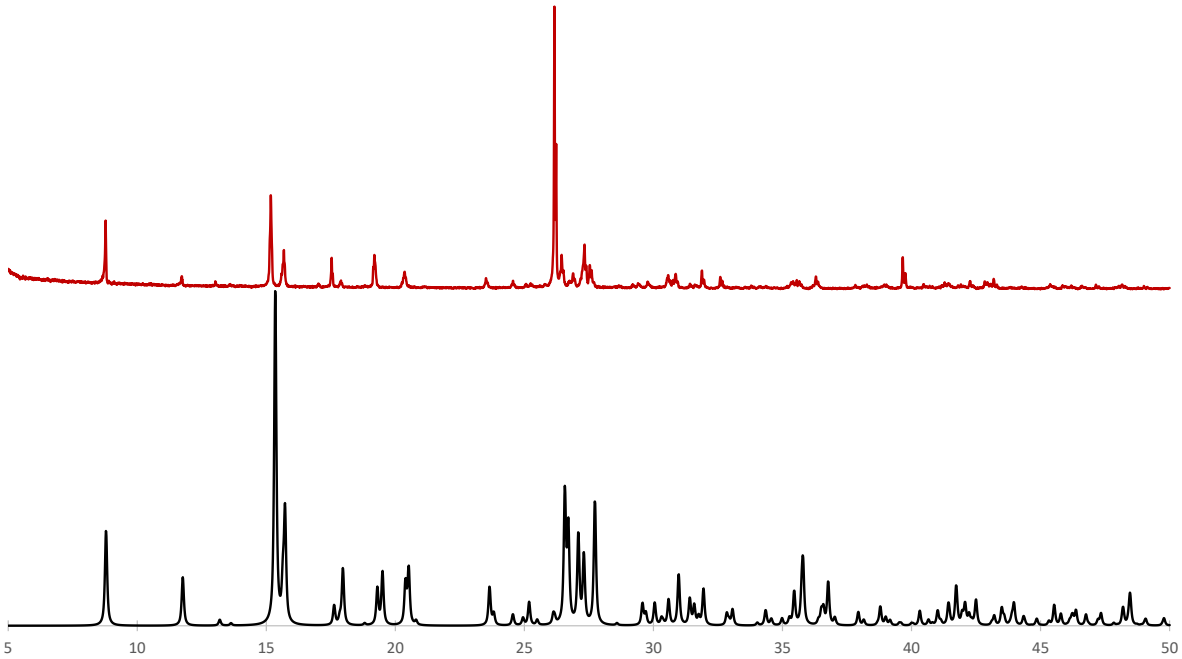

Figure S22. Experimental (red) and simulated (black) PXRD patterns of **6a**.

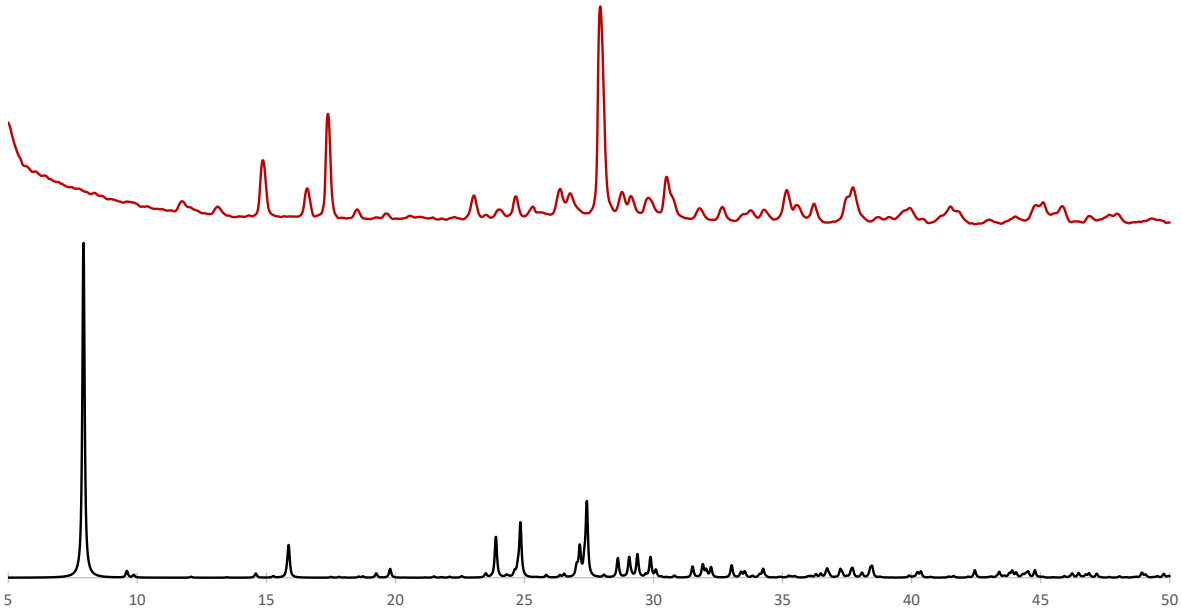

Figure S23. Experimental (red) and simulated (black) PXRD patterns of **6b**.

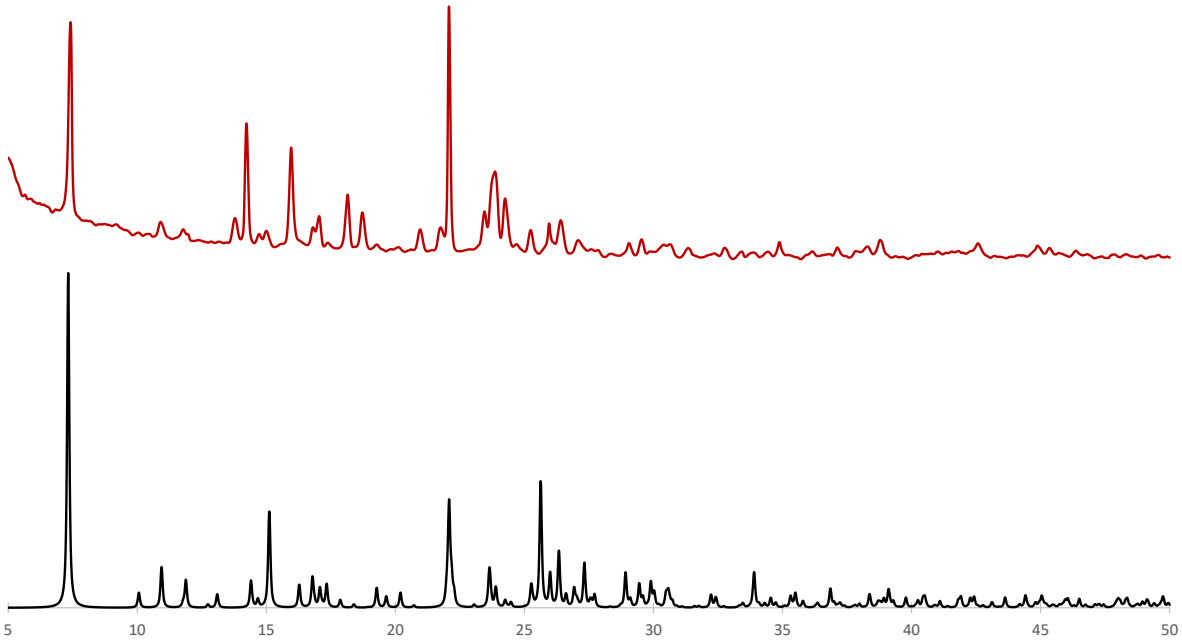

Figure S24. Experimental (red) and simulated (black) PXRD patterns of **7**.

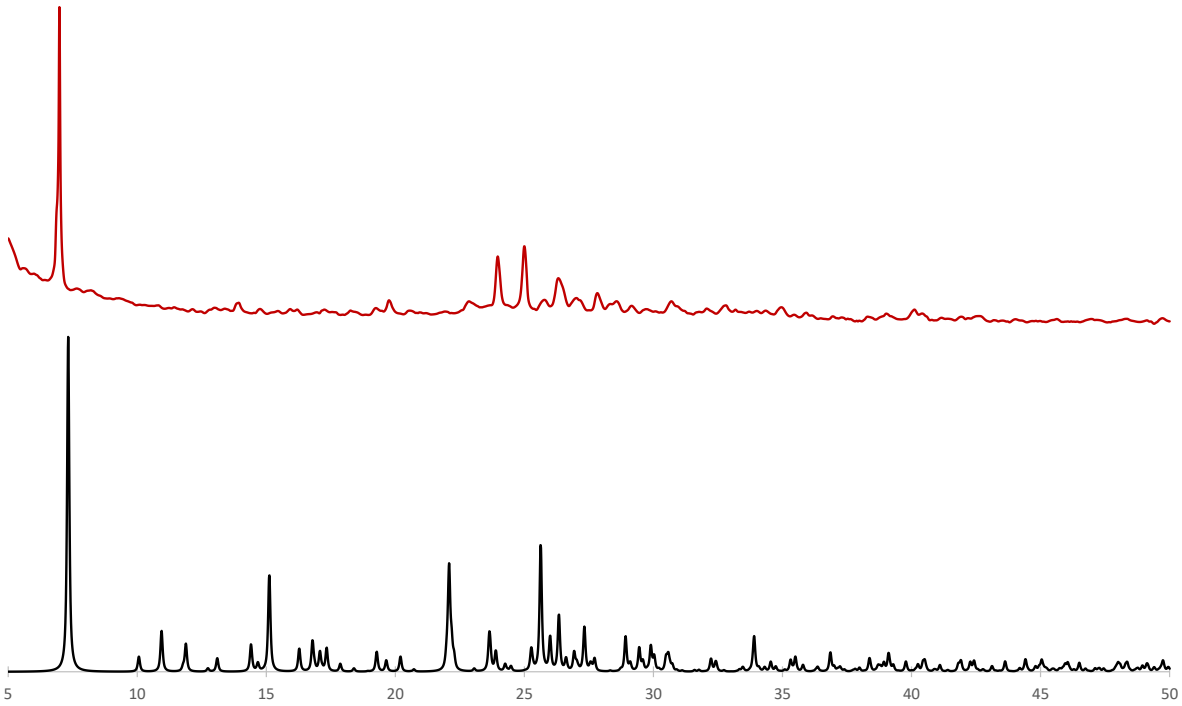

Figure S25. Experimental (red) and simulated (black) PXRD patterns of **8**.

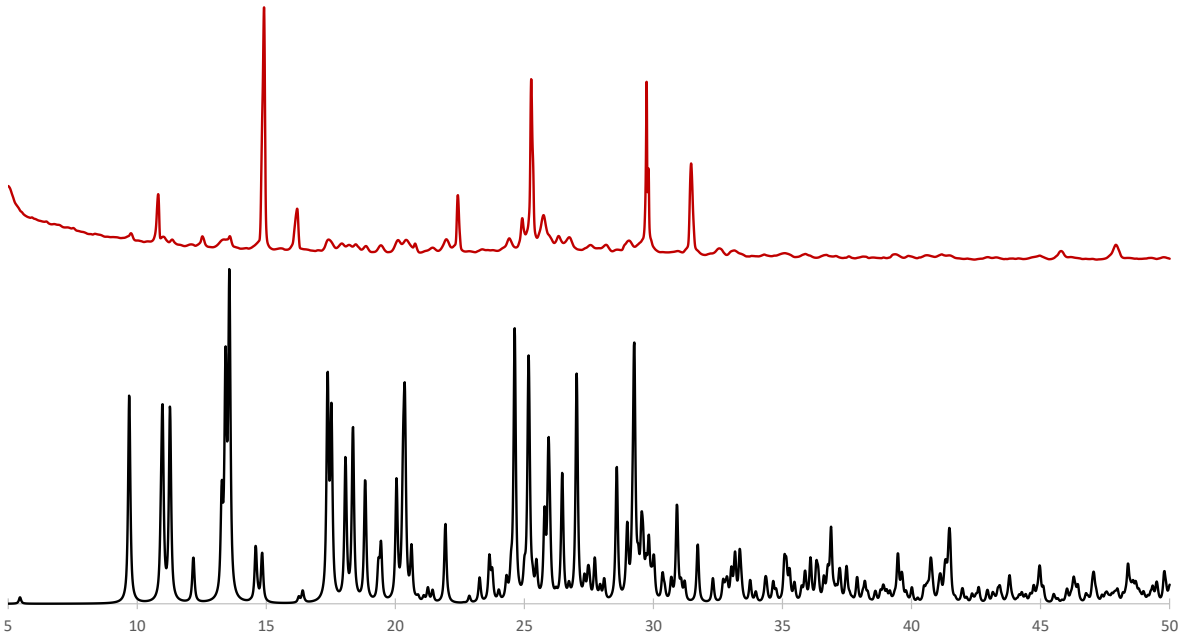

Figure S26. Experimental (red) and simulated (black) PXRD patterns of **9a**.

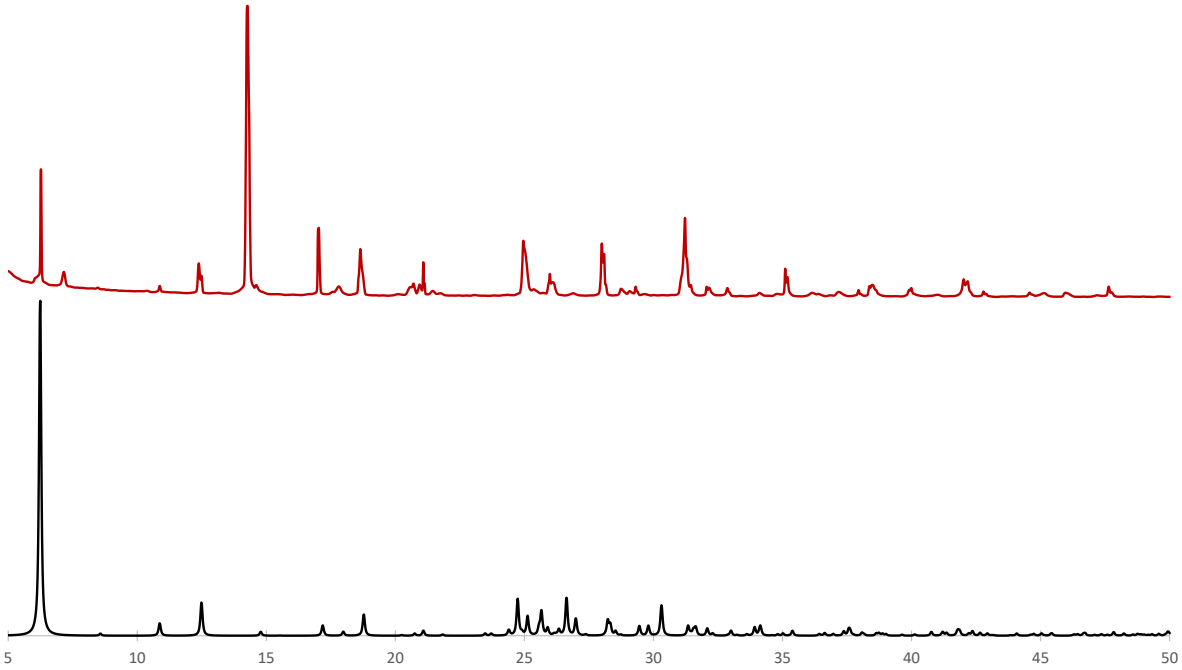

Figure S27. Experimental (red) and simulated (black) PXRD patterns of **9b**.

References

[S1] Pilgram K., Zupan M., Skiles R., *J. Heterocycl. Chem.*, **1970**, *7*, 629–633.

[S2] Eichstaedt K., Wasilewska A., Wicher B., Gdaniec M., Połoński T., *Cryst. Growth Des.*, **2016**, *16*, 1282–1293.

[S3] Centore R., Borbone F., Carella A., Causà M., Fusco S., Gentile F.S., Parisi E., *Cryst. Growth Des.*, **2020**, *20*, 1229–1236.

[S4] Parsons S., Flack H.D., Wagner T., *Acta Crystallogr. Sect. B* , **2013**, *69*, 249–259.